3D geomechanical analysis of rock mass stability of the Spiš Castle (Slovakia) using high-resolution point cloud data

Martin Maľa*, Vladimí Greif & Ján Vlčko

Comenius University Bratislava, Faculty of Natural Sciences, Department of Engineering Geology, Hydrogeology and Applied Geophysics, Ilkovičova 6, 842 15 Bratislava, Slovakia; mala26@uniba.sk, vladimir.greif@uniba.sk, jan.vlcko@uniba.sk

* Corresponding author

AGEOS

Abstract: Conventional surveying techniques frequently prove inadequate in providing a detailed geomechanical assessment of rock masses, particularly in evaluating stability concerns related to culturally significant hilltop structures. At Spiš Castle in Eastern Slovakia the drone obtained high-resolution 3D point cloud data were employed to overcome these limitations, offering enhanced insight into the structural and kinematic characteristics of the underlying travertine mound. This approach enabled precise extraction of discontinuity geometries and facilitated identification of key instability mechanisms that may pose a threat to historical buildings, especially on the eastern and northern flanks of the site. The spatial distribution and orientation of discontinuities manifest a systematic pattern indicative of tectonic origin, which persists in influencing the mechanical integrity of the rock mass. A significant number of discontinuities meet the geometric prerequisites for planar failure, suggesting a conditional stability state that could be compromised by minor external disturbances. Although current evidence signifies minimal mass movement and an overall stable condition, the analysis identified several potentially unstable blocks. While these blocks do not pose an immediate threat, their structural context and vulnerability to climate-induced stressors emphasise the necessity of continuous monitoring and re-evaluation. These findings highlight the value of remote sensing technologies in evaluating long-term geohazards threatening heritage sites.

Keywords: Rock mass stability, Cultural Heritage, Spiš Castle, Remote sensing, Structural Analysis, Kinematic Analysis

1. INTRODUCTION

Natural hazards like slope deformations pose a threat not only to human life and modern infrastructure (Bell & Glade, 2004), but also to cultural landmarks that have been bequeathed to us by previous generations (Nicu, 2017). These heritage sites are of paramount importance as they serve as a crucial link to our past, reflecting the beliefs and traditions of earlier societies, and serving as powerful symbols of our cultural identity. The impact of slope deformations on cultural heritage is a multidisciplinary theme that typically necessitates a distinct methodological approach (Canuti et al., 2009). Comprehensive research is frequently found upon the analysis of geotechnical, structural, and engineering problems and should lead to the design of appropriate countermeasures (Fanti et al.2013; Pagliarulo & Parise, 2000; Cotecchia et al., 2005; Gutierrez, 2010; Gutierrez et al., 2014)).

In the territory of the Slovak Republic, one such historical monument is Spiš Castle, which is an important national cultural monument, and a UNESCO World Heritage Site, which represents a breathtaking medieval fortification in Central Europe. Spanning an impressive 3.9 hectares, the castle is considered one of the largest medieval complexes in Central Europe (Vlčko et al. 2009). The castle's origins date back to 1120, and its history is marked by a complex architectural evolution. Major construction phases began in the early 13th century showcasing remarkable craftsmanship and strategic design. However, a devastating fire in 1780 left the castle in ruins, making it the largest such site in Slovakia. Efforts to preserve and partially reconstruct surviving structures began in the 1960s, driven by the urgent need to halt its natural deterioration.

From a geological perspective, Spiš Castle is situated atop a travertine mound called Dreveník, which is underlain by Paleogene sediments comprising claystone and sandstone layers in a flysch-like formation (Malgot et al., 1992). The geological foundation of the area renders it susceptible to slope deformations,including block movements, rockfalls, and landslides. It is noteworthy that karst processes, erosion, and weathering contribute significantly to the degradation of the travertine mound (Ivan, 1943; Vítek,1970; Cebecauer,1972, Gutierrez, 2010; Gutierrez et al., 2014; Parise et al., 2015). Svatoš (1970) provided a detailed analysis of the Dreveník travertine, identifying an intricate network of cracks and fissures through the interpretation of aerial photographs. Subsequent studies, including those by Nemčok and Svatoš (1974), documented the gravitational disintegration of the mound, while Nemčok (1982) elaborated on faulting mechanisms in the region. Based on these findings, it can be concluded that the primary deformation mechanism affecting the Dreveník travertine mound is lateral spreading. Lateral spreading is classified as a type of deep-seated gravitational slope deformation (DSGSD) a process widely documented in international literature, particularly in carbonate and karst environments (Gutierrez et al., 2014; Parise et al., 2015). Pánek and Klimeš (2016) state that the term was first introduced by Malgot (1977) to describe large-scale slope deformations induced by gravitational loosening of brittle, neovolcanic rocks situated above Palaeogene and Neogene rocks in the Western Carpathians of Slovakia.

Spiš Castle represents a very interesting case in the field of slope instability; however, the significance is not only associated with the historical relevance of the site and of its monuments

Manuscript received 2026-04-23
Revised version accepted 2026-06-12

Fig. 1. Dividing the eastern side of Spiš Castle into the eastern respectively northern section.

but also with the implementation of an integrated approach of different techniques of geomechanical investigation and data collection presented in this manuscript. Similar integrated approaches combining engineering geology, structural analysis, and advanced 3D data acquisition techniques have been successfully applied at unstable cultural heritage sites worldwide (Pagano et al., 2020; Cardia et al., 2023; Cardia et al., 2024). Currently, Spiš Castle is undergoing a comprehensive reconstruction, overseen by the Slovak National Museum and divided into five stages. This initiative comprises an engineering-geological survey of the travertine mound situated beneath the eastern palaces. The utilisation of high-resolution point cloud data has enabled a three-dimensional analysis of both structural and kinematic conditions. The study's objective is to identify sections of the bedrock that are susceptible to instability and evaluate the efficacy of past remediation measures. The objective is to provide information that will contribute to the development of stabilization strategies that will mitigate the risks posed by slope deformations to the castle's structure. This multidisciplinary approach highlights the interconnectivity of geological, architectural, and environmental factors in preserving one of Slovakia's most iconic cultural landmarks. The research aims to address pivotal questions pertaining to the physical condition of the bedrock, the efficacy of previous interventions on the travertine mound's stability consistent with studies on hazard assessment and risk mitigation in karst environments (Gutierrez, 2010; Gutierrez et al., 2014; Parise et al., 2015). The insights gained will contribute to the sustainable preservation of Spiš Castle and its surrounding landscape.

2. METHODS

2.1 Structural and kinematic analysis

As the orientation of the fractures within travertine mound isn't random, but related to the tectonic processes a structural and kinematic analysis can be very useful in the identification of the bedrock sectors which can be more prone to instability processes.

Prior to the analysis the bedrock beneath the eastern palaces of Spiš Castle was photographed using UAV (DJI Mini 3 Pro) photogrammetry. This non-contact, non-destructive method captures the rock mass surface using a series of aerial images and by processing it one obtains a high-resolution digital replica of the rock slopes. GPS-integrated drones provided precise spatial coordinates (X, Y, Z, S-JTSK) and color data (RGB) for each point. The processed point cloud, consisting of over 30 million points (cloud density of the rock surface areas was approx. 450 points/m^2), enabled detailed structural analysis, including the measurement of 9,817 discontinuity surfaces meeting kinematic analysis criteria using SpitFX software.

Discontinuity orientations were determined using specialized software for 3D point clouds and supplemented by manual measurements with a geological compass at accessible locations. The study area, spanning from the Romanesque Palace in the North to the eastern palaces, was divided into east and north sections (Figs. 1 and 2). A statistical analysis of discontinuities was performed using tectonograms in Schmidt projections, with results visualized on a colored point cloud or a triangular grid. These findings formed the basis for a kinematic stability analysis, representing the initial step in assessing the stability of the rock mass.

Kinematic analysis serves as a preliminary tool for assessing the kinematic possibility of three major rock mass failure mechanisms, including:

- Planar sliding (Hoek & Bray, 1981; Goodman, 1980);
- Wedge failure (Hudson & Harrison, 1977);
- Flexural toppling (Goodman & Bray, 1976).

This was achieved by analyzing the orientation of discontinuities in stereographic projection relative to slope orientation and the internal friction angle at fractures.

Kinematic analysis for planar sliding is a process of determining the feasibility of slippage occurring along a single shear surface, in relation to the angle of internal friction. The resultant

Fig.2. The following visual representation illustrates the 3D point cloud, showcasing the rock slopes situated at the base of the eastern palaces within the surveyed section of Spiš Castle. Discontinuities in the rock massif are marked in color.

tectonogram delineates a hazardous area (red area) in which the poles of discontinuities with orientations falling within this area are susceptible to planar failure (see Figure 3A). In accordance with the work of Goodman (1976), lateral limits are applied for planar failure, beyond which slip will no longer occur because of the large deviation of the azimuths of the discontinuities from the direction of the rock slope.

Conversely, the kinematic analysis for wedge sliding explores the potential for shear failure of blocks resulting from the intersection of two discontinuities, with respect to the slope orientation and the angle of internal friction at the fissures. As demonstrated in Figure 3B, the intersection of discontinuities falling within the red region are susceptible to this particular form of failure. It is imperative to acknowledge that the kinematic analysis systematically relocates all discontinuities to the center of the projection, thereby simplifying the representation to a single location. However, this does not accurately reflect the actual conditions present in the slope, consequently leading to the erroneous assumption that not all fault ruptures must occur in reality.

The kinematic analysis for toppling is an assessment of the possibility of toppling blocks according to the conditions described in Hudson and Harrison (1997). The fundamental characteristics that are conducive to this particular form of failure can be categorized as follows: the existence of two systems of discontinuities whose intersections exhibit a concave curvature in the direction of the slope, thereby forming discrete blocks; and the presence of a third system of discontinuities that separates the blocks, enabling them to rotate or shear along the base. The resulting tectonogram is delineated by three critical zones (Fig. 3C). It is widely accepted that zones 1 and 2 are the so-called primary critical zones. In these zones, the intersections of the discontinuities fitting into the slope are within the lateral limits, and this is similar to planar sliding. It is important to note that the blocks in zone 2 have a steeper slope, which increases the risk of toppling in comparison to zone 1. Zone 3 (yellow area) is also referred to as oblique toppling, and it has been determined that blocks with near vertical orientations of the bounding discontinuities are capable of toppling even at larger deviations from the slope dip direction. In zones 2 and 3, the intersection of discontinuities is localized within the shear cone, thereby rendering the basal surface immobile due to friction. However, rotational movement remains possible.

2.2 Rock mass mechanical properties

In order to ascertain the fundamental parameters of rock properties necessary to meet the objectives of the engineering geological survey and slope stability analysis, rock samples were obtained from rock blocks extracted directly on the site. Two travertine monoliths were sampled front the eastern wall of the castle rock, from which test specimens were cut in the necessary dimensions and number for the determination of individual characteristics - the bulk density of the rock and shear parameters on rock discontinuities.

Bulk density

The bulk density of the rock samples was determined by measuring the mass of a known volume of the samples, which were adjusted to the shape of cylinders with a diameter of 50 mm and the same height, according to STN EN 1097-6 (2014). The samples were weighed in a dry state, following which they were submerged in water. The bulk weight of the aggregate was calculated according to the following formula:

$$\rho_d = \frac{m_d}{m_d - m_h} \tag{1}$$

where, ρ_d is bulk density of the dried sample [g.cm^{-3}]; m_d is mass of the specimen [g] and m_h is mass of the specimen immersed in water [g]. Test results of 5 specimens are in table.1.

Shear strength of rocks

Samples were prepared from drill cores, with the shear surface positioned in the plane of contact between the upper and lower

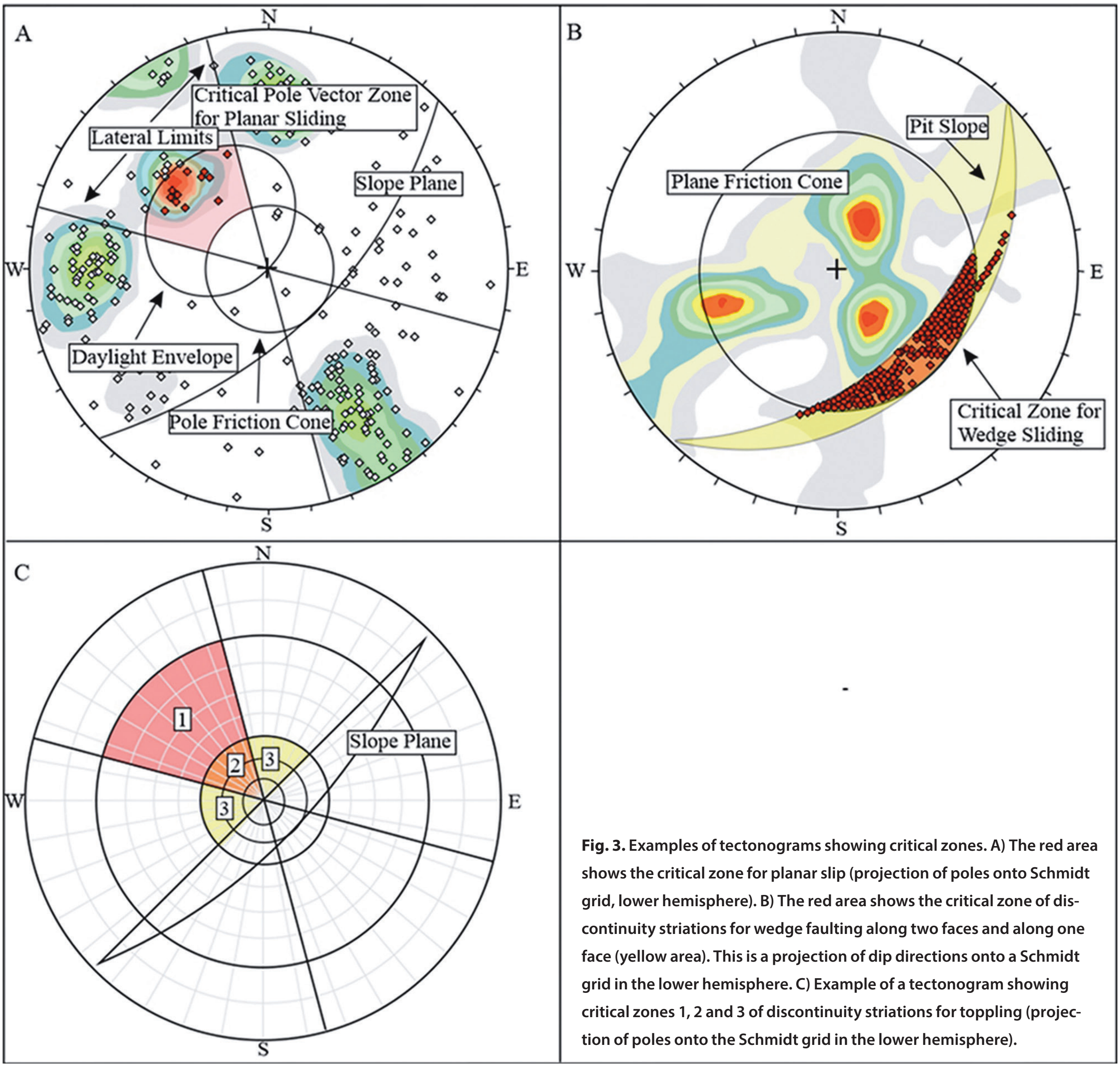

Fig. 3. Examples of tectonograms showing critical zones. A) The red area shows the critical zone for planar slip (projection of poles onto Schmidt grid, lower hemisphere). B) The red area shows the critical zone of discontinuity striations for wedge faulting along two faces and along one face (yellow area). This is a projection of dip directions onto a Schmidt grid in the lower hemisphere. C) Example of a tectonogram showing critical zones 1, 2 and 3 of discontinuity striations for toppling (projection of poles onto the Schmidt grid in the lower hemisphere).

Tab. 1. Bulk density of the tested travertine

Specimen	Bulk density (g.cm^{-3})
T1	2,5192
T2	2,489
T3	2,504
T4	2,4915
T5	2,559
Average Value	2,5125

jaws of the shear apparatus. This was ensured by plastering the specimen with high-strength gypsum using a mould supplied by the shear apparatus manufacturer, with the specimen halves temporarily joined by a wire which was removed just prior to the test.

Prior to the commencement of the test, the test specimen was meticulously documented. Both contact surfaces of the specimen were photographed, the area was calculated, and a record of the surface roughness of the discontinuity surfaces was made with a profilometer. Thereafter, the joint roughness coefficient (JRC) was determined. The magnitude of the shear strength on the discontinuities is contingent on the surface roughness, which is primarily determined by the lithological nature of the rock (Zheng, 2020).

To determine the residual friction angle of the travertine, reference specimens with artificially sawn (smooth) shear surfaces were prepared and tested. Rock friction angle was determined acording to the Eq.2. as follows:

$$ {}_r = ({}_b - 20) + 20\left(\frac{r}{R}\right) \qquad (2) $$

where r is the Schmidt rebound number for wet and weathered fracture surfaces and R is the Schmidt rebound number for dry, unweathered, sawn surfaces.

The roughness expressed by JRC is incorporated into the calculation of the shear strength of discontinuities using the

Barton-Bandis criterion (Barton, 1976), in conjunction with the discontinuity strength of JCS and the determined value of the residual shear strength φ_r.

$$\tau = \sigma_n \tan\left({}_r + JRC\log_{10}\left(\frac{JCS}{\sigma_n}\right)\right) \qquad (3)$$

The specimen, was then subjected to a normal force of 2.5, 5, 10 and 15 kN, respectively, using a shear apparatus. During the experimental procedure, the tangential force was increased incrementally until a sustained motion (shear) along the discontinuity was observed. During the experimental procedure, the magnitude of displacement, tangential force and normal force were recorded. The determination of peak and residual values of shear strength was made from the test record plotted using a plot of tangential stress versus displacement. The test was performed at four different normal stresses, enabling the shear strength line to be plotted and the shear strength parameter to be determined. This parameter includes the shear strength angle φ_0 (φ) and the initial shear strength τ_0 (c) [kPa].

2.3 Slope stability analysis

The potential instability of rock blocks was identified through a combination of field reconnaissance, the analysis of video footage obtained from the drone, and 3D point cloud analysis. The computational sections were routed through them, in which stability degree calculations were performed.

Stability calculations were performed using RockPlane, a commercial software program developed by GeoStru. This software facilitates the calculation of the stability of rock blocks of a given shape. This fact is mentioned merely because, to date, no software has been developed to calculate unstable rock blocks that have an overhanging shape (convex shape). The calculation was based on real input data, i.e. the shape and orientation of the discontinuities defining the unstable block were read from a 3D point cloud, while the shear parameters and the bulk density represent input data obtained by laboratory tests. The calculation was conducted under static conditions. The calculation was based on the long-term stability conditions, which are defined as the value of the stability degree Fs=1.5. Consequently, the primary focus of this study was to ascertain the resultant force necessary to ensure the desired level of stability.

A stability level value of less than 1 indicates that the block is unstable. Values ranging from 1 to 1.5 signify that the block is stable, but that some form of stabilisation intervention will be required in the long term. Eight sections, each characterised by the presence of larger-dimensional blocks, were selected for the calculation (Fig. 4). For three of these blocks (BL3, BL6, BL7), the calculation was conducted with embedded steel bolts. This approach was adopted since it was found during the survey that these bolts were already anchored, thereby demonstrating their long-term effectiveness. Due to the absence of the original technical documentation from the 1990s stabilization project, standard conservative parameters for historical systematic anchor rods were assumed (diameter of 25 mm, tensile strength of 570 MPa, and length of 4 m) to perform back-analysis.

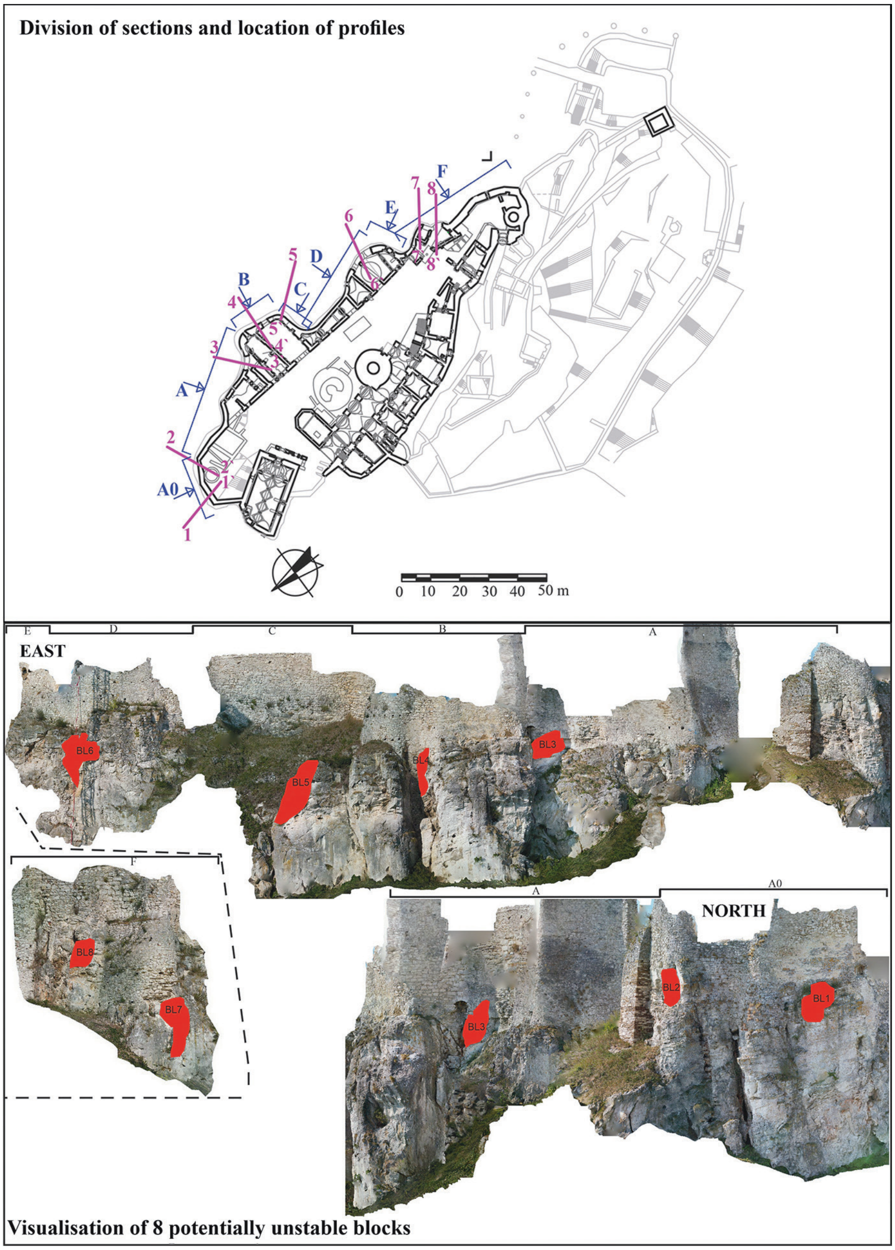

Fig. 4. Division of sections and location of profiles (up); 3D visualisation of 8 potentially unstable blocks (down)

3. RESULTS

3.1 Shear strength of the rock mass

The final peak shear strength-peak shear stress parameters at the characteristic normal stress of specimens SP-1 and SP-2 are given in Tables 2 and 3, respectively. Figure 5 plots the actual test runs as well as the shear strength curves.

Tab. 2. Peak shear stress, sample SP-1

Normal force [kN]	Peak Shear Froce [kN]	Normal stress [kPa]	Peak Shear stress [kPa]
15	12.60	2855	2398
10	8.70	1903	1656
5	4.90	1047	932
2.5	2.90	457	552

Tab. 3. Peak shear stress, sample SP-2

Normal force [kN]	Peak Shear Froce [kN]	Normal stress [kPa]	Peak Shear stress [kPa]
15	12.60	2855	2437
10	8.70	1903	1584
5	4.90	1047	975
2.5	2.90	457	457

The mean values of shear angle φ_0 (°) and initial shear strength τ_0 (c) [kPa] have been determined for a residual friction angle $\varphi_r = 37°$ and values JRC (3) and JCS (45 MPa) in accordance with ASTM D5607 and ISRM and are presented here for reference $\varphi = 43°$ and c=3 kPa. The resulting values were calculated as the arithmetic mean of the tested specimens. The variation in cohesion values for the test specimens is attributable to the disparate surface roughness of the crack surfaces tested.

3.2 Structural and Kinematic Analyses

The processing of discontinuities was undertaken on the basis of a structural analysis of such features, with both those detected automatically by a special algorithm and those identified manually in the processed point cloud. These discontinuities were then combined into surfaces, the orientation of whose dip/dip direction was statistically processed into a tectonogram using Schmidt projection into the lower hemisphere (Fig. 6). A Schmidt projection is a Lambert azimuthal equal-area projection of the lower hemisphere onto the plane of a meridian. The following section presents the findings of the structural analysis for the eastern and northern region.

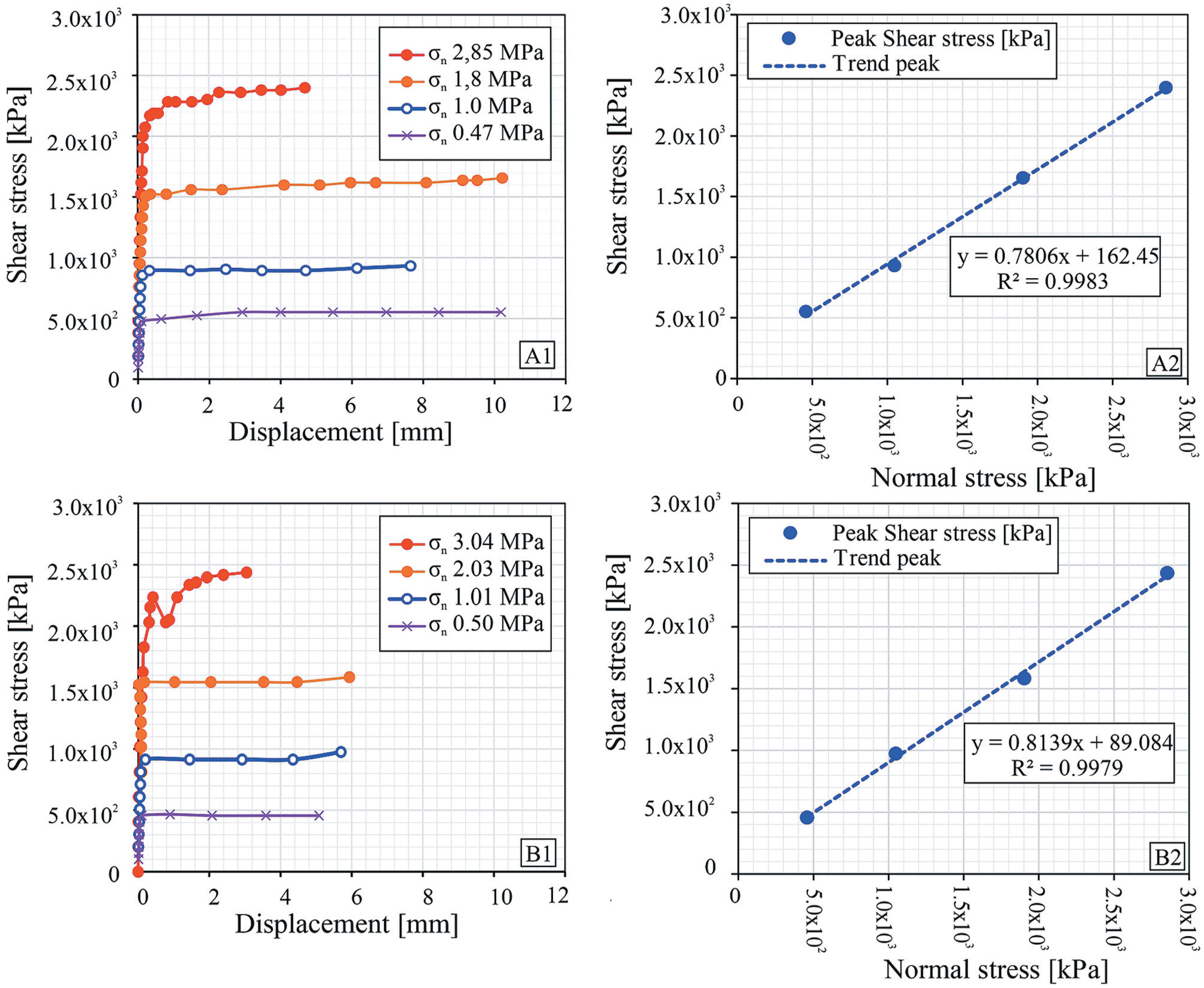

Fig. 5. A1: Shear stress vs Displacement, SP-1-; A2: Shear strength curve of specimen SP-1;B1: Shear stress vs Displacement, SP-2-; B2: Shear strength curve of specimen SP-2

3.3 Structural analysis- East and North

The selection of discontinuities was based on an analysis of the orientation of the discontinuities (dip direction/dip) in relation to the slope orientation. This analysis was conducted on the entire eastern and northern side of the travertine bedrock The selection process involved the utilisation of a substantial amount of data (discontinuity poles). The data were then displayed in the form of a tectonogram. The tectonogram was based on an equal-area projection (Schmidt) with a projection into the lower hemisphere. From this number, a kinematic analysis has been developed for the three basic types of failure mechanisms in rock masses, i.e. planar sliding, wedge failure and toppling. This analysis is based on the above-described parameters, such as the orientation of discontinuities, the slope orientation, the friction angle of discontinuities, as well as other input parameters for each type of discontinuity (e.g., lateral limits for planar sliding, etc.).

As illustrated in Fig. 6, the discontinuities were categorized into six systems throughout the east and north side of the travertine bedrock.:

- System 1m - 136/87 - tectonic discontinuities
- System 2m - 177/84 - tectonic discontinuities
- System 3m - 227/78 - tectonic discontinuities
- System 4m - 261/90 - tectonic discontinuities
- System 5m - 101/16 – stratification
- System 6m - 249/52 - tectonic discontinuities, lower gradient

Based on the average dip/dip direction data from all six systems, it is striking that there is some regularity in the orientation of the discontinuities, and that the orientations are likely to be

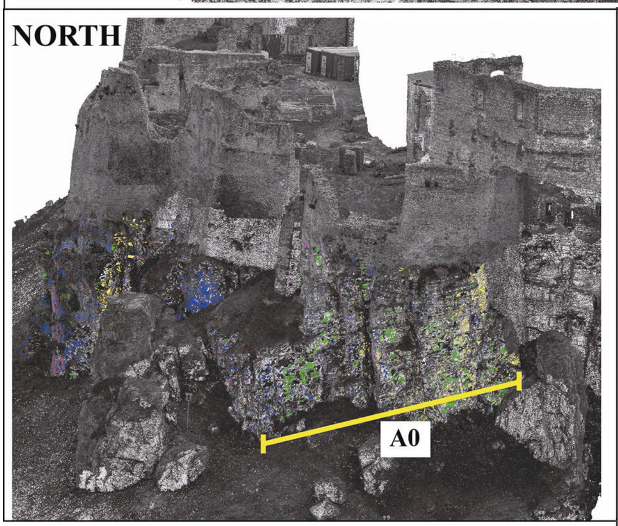

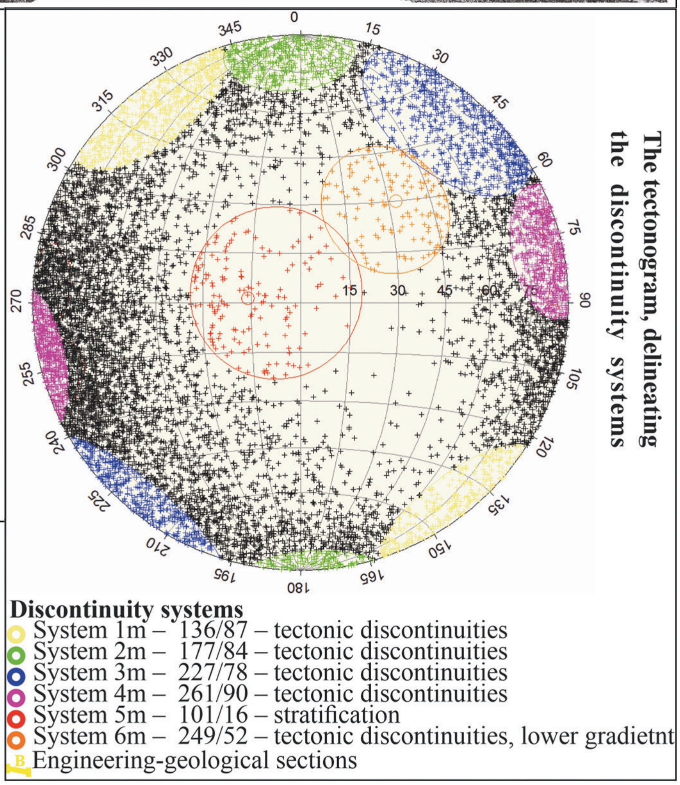

Fig. 6. Results of structural analysis for north resp. east section of the travertine mound with discontinuity system classification

repeated over the extent of the entire cliff, if not in addition to the extent of the bedrock that we examined from the studied north and east sides.

3.4 Kinematic analysis-East

A thorough kinematic investigation was conducted for the eastern segment of the Spišský hrad bedrock, encompassing planar sliding, wedge failure, and toppling phenomena. The analysis for planar sliding (Fig. 7) was based on a representative slope orientation of 89°/87°, corresponding to the average orientation of exposed rock faces in this part of the slope. The angle of internal friction along discontinuities was set at 43°, based on direct shear test results. It was determined that planar failure was a possibility along steeply inclined discontinuities of the 4m system, with orientations ranging from 70–110°/45–85°. These correspond to 634 discontinuities, accounting for 35.52% of the 4m system. Of the total of 7141 mapped discontinuities, 1770 (equaling 24.79%) fall within the critical range for planar sliding. It is important to note that this group may include both currently active and previously failed surfaces. Conversely, discontinuities inclined at less than 43° have been shown to be stable, due to an insufficient driving force for slip.

The wedge failure analysis was performed for the same slope and friction parameters. Due to the substantial number of intersections among discontinuities, the analysis concentrated on the averaged orientations of systems 1m and 6m. The results are presented in a manner that is distinct from that of other analyses, in that they are displayed as slope-vector projections of the six main discontinuity groups. As demonstrated in Fig.7 a mere 15 intersections of the great circles are situated within the critical zone for wedge failure, predominantly involving interactions between the 1m and 2m systems. However, it was found that only one intersection cluster, representing 6.67% of the total number of discontinuities considered, was classified as critical. Although geometrically feasible, wedge failure is therefore assessed as having minimal significance in this zone.

Utilising the identical parameters, a toppling analysis was conducted, which revealed that 2068 discontinuities (28.96%) satisfied the geometric criteria for potential toppling. These are predominantly associated with the 5m and 4m systems. The 5m system (101/16) incorporates 97 critical basal discontinuities (85.09% risk within that group), while the 4m system (261/90°) comprises 697 critical discontinuities (39.05% risk) (Fig. 7). Full toppling criteria were met in 15 cases, as indicated by orange points in Fig. 7, where intersecting discontinuity systems create isolated blocks inclined towards the slope. However, it is important to note that only one of these cases is considered critical, and this occurs in region 2 (the "shear cone"), where basal sliding is restricted by friction, although rotational motion remains possible. Furthermore, shear toppling was initiated at four of the 15 intersections (26.67%) in zone 3, where the slope geometry allows overturning even at greater angular deviations from the slope face. Despite this, both direct and oblique toppling in the eastern section appear improbable under current conditions, indicating that structural stability is maintained and that failure by toppling is not expected to manifest.

3.5 Kinematic analysis-North

The kinematic analysis for planar sliding in the northern bedrock segment (Fig. 8) was conducted using a slope orientation of 10°/88° and an internal friction angle of 43°, consistent with the eastern section. Planar sliding in this region is predominantly associated with steeply inclined discontinuities of the 2m system, exhibiting orientations ranging from 350–40°/45–88°. This subset comprises 521 discontinuities, accounting for 19.47% of the 2m system, of which 217 (28.63%) are considered critical for planar sliding. Like the east side, this group may include surfaces where past slip and subsequent block collapse have occurred. Conversely, discontinuities with inclinations below the friction angle (43°) are assumed to be stable under current conditions.

The wedge failure analysis for the northern section utilized the same parameters as the planar sliding analysis. Due to the high number of discontinuity intersections, the analysis was restricted to mean orientations of the six primary systems (1m–6m). Tectonograms are presented as averaged slope vector projections rather than individual poles. As demonstrated in Fig.8, a mere 15 great circle intersections fall within the theoretical failure zone, and none of these represent true intersections of discontinuities. This finding indicates that there are no critical cases and confirms that wedge failure is not a concern in this particular region of bedrock. Consequently, the northern part of the bedrock is regarded as structurally stable with respect to wedge failure .

The toppling analysis was performed using the same input parameters. Amongst the 2676 identified discontinuities, 653 (24.40%) show orientations that are susceptible to toppling, primarily within the 5m and 2m systems. The 5m system (101°/16°) encompasses 97 critical discontinuities, signifying a 66.04% toppling risk within that group. In contrast, the 2m system (177/84°) consists of 233 critical joints (30.74%), as illustrated in Fig.8. It is noteworthy that full geometric conditions for toppling, that is to say, intersecting discontinuity sets forming discrete blocks dipping towards the slope, were fulfilled in 15 instances (illustrated as orange dots in Fig.8). However, only two of these (13.3%) fall into region 2 (the shear cone), where basal sliding is impeded by friction, though rotational movement remains possible. Furthermore, 40.00% of the intersections (six in total) are located within zone 3 (illustrated as the yellow area in Fig.8), where conditions are prone to oblique toppling. It is noteworthy that blocks in this zone have the potential to overturn even at greater angular deviations from the slope direction. Notwithstanding these findings, the potential for both conventional and oblique toppling in the northern segment remains minimal, thereby substantiating the conclusion that this area is geotechnically secure.

The results obtained demonstrate the theoretical viability of the analysed failure mechanisms. Of these, planar sliding poses the greatest risk in the eastern and northern sectors, while wedge failure and toppling are largely confined to isolated or marginally critical cases.

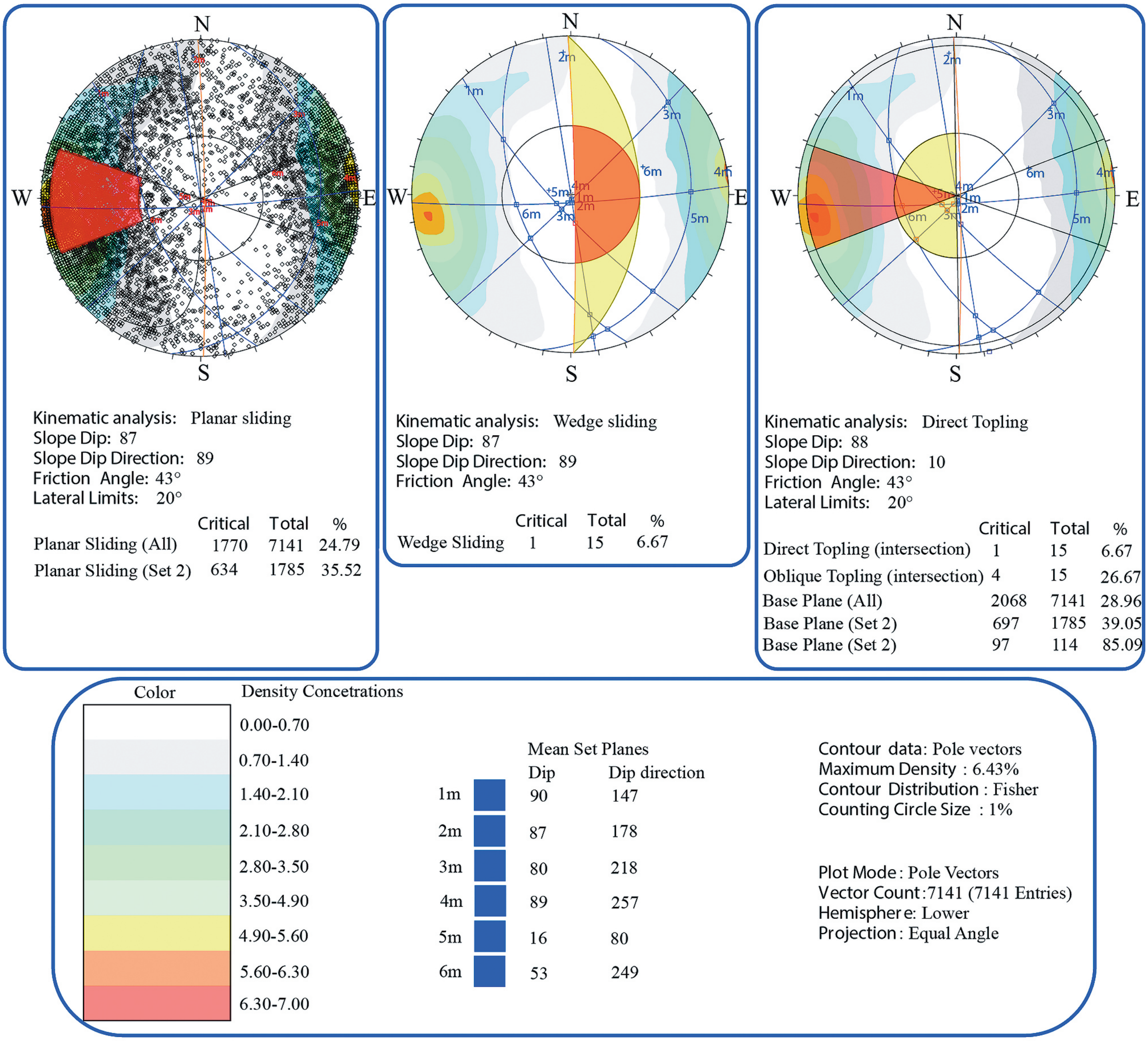

Fig. 7. Results of kinematic analysis for planar sliding; wedge sliding; direct topling- east section

Tab. 4. Results of stability calculations for blocks BL1-BL8

Block	Degree of stability
BL1	5.146
BL2	5.092
BL3	3.021
BL4	1.272
BL5	1.283
BL6	3.438
BL7	5.238
BL8	1.345

3.6 Results of rock block stability calculations

As previously mentioned in the methods section, a total of eight potentially unstable blocks (BL-1 to BL-8) were identified in the initial phase of the field engineering geological survey, which could also affect the stability of the outer walls of Spiš Castle in the event of their displacement. As is evident from Table 4. that the blocks designated BL1; BL2; BL3; BL6 and BL7 have a degree of stability Fs that is significantly higher than the required degree Fs = 1.5. This finding indicates that these blocks do not require any stabilisation. It is evident that the blocks BL4 (Fs=1.272), BL5 (Fs=1.283) and BL8 (Fs=1.345) exhibit a degree of stability that is lower than the requisite value for ensuring long-term stability. It is acknowledged that these blocks do not pose a significant threat to the castle walls or visitors to this historical monument; consequently, their value is deemed adequate.

4. DISCUSSION AND CONCLUSION

The results of the structural and kinematic analyses provide a comprehensive understanding of the rock mass behavior on the eastern and northern faces of the Spišský hrad bedrock. The dominance of planar sliding mechanisms, particularly in steeply inclined

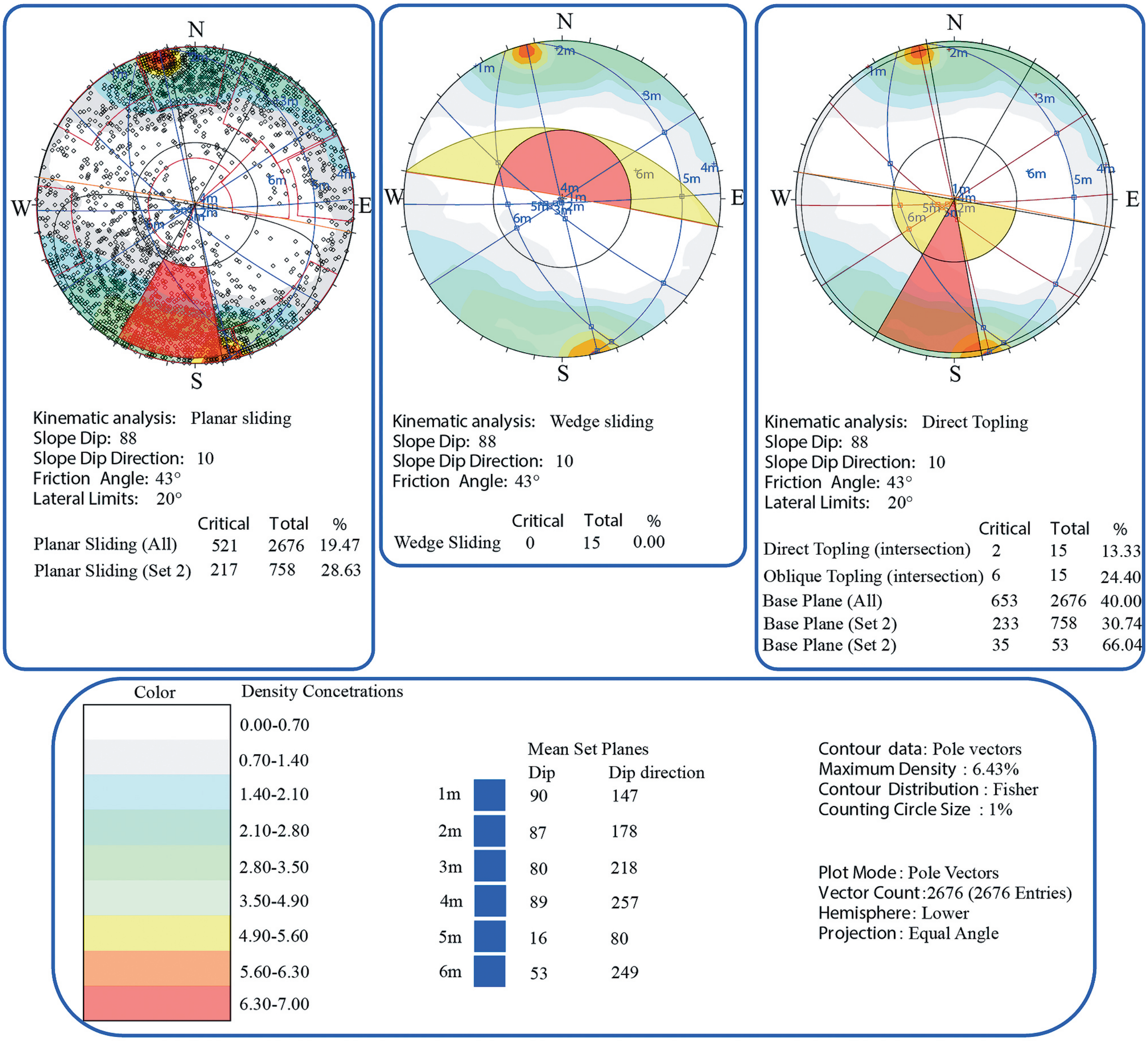

Fig. 8. Results of kinematic analysis for planar sliding; wedge sliding; direct topling- north section

discontinuity systems such as 4m and 2m, underscores the pivotal role of orientation and frictional properties in ensuring slope stability. Although wedge failure and toppling appear to be geometrically possible, they are mostly confined to isolated instances with limited geotechnical relevance under current conditions.

A noteworthy discovery is the considerable proportion of discontinuities that satisfy the geometric criteria for failure, particularly regarding planar sliding. This suggests that while the current stability of the rock mass is generally acceptable, even minor perturbations (e.g., seismic loading, freeze-thaw cycling, or anthropogenic vibrations) could lead to localized failures. The identification of critical blocks with stability factors that are slightly below the threshold value of Fs = 1.5 provides further evidence for the necessity of long-term monitoring, particularly in the context of changing climatic conditions.

The discontinuity patterns observed in both regions manifest regularity, thus suggesting a tectonic origin that continues to exert influence on the mechanical behavior of the rock mass. These observations are consistent with regional structural trends reported in previous works on Central European Neogene travertines (Malgot et al., 1992; Nemčok, 1982; Malgot, 1977). Furthermore, the relatively increased cohesion and internal friction values derived from direct shear testing serve to confirm the mechanical robustness of the intact travertine. However, it should be noted that surface weathering and sub-surface alteration have the potential to locally reduce strength parameters over time.

It is important to note that the current evidence of mass movement is limited, which suggests that active deformation is minimal. However, latent instabilities have been identified, particularly in blocks BL4, BL5, and BL8. While these blocks are currently deemed non-critical, they should be considered for periodic reassessment, particularly in light of increasing climatic extremes. Freeze-thaw cycles, a common occurrence in this region, have been demonstrated (Maľa et al., 2021; Maľa et al., 2024) to contribute to progressive weakening of joint walls, ultimately reducing resistance to sliding or overturning.

In the context of cultural heritage preservation, the stability of these blocks assumes added importance. Spiš Castle is a nationally significant site and is subject to frequent visitor traffic and exposure to environmental stressors. Consequently, even low-probability failure mechanisms could have disproportionately high consequences. The implementation of a monitoring program, incorporating ground-based LiDAR, extensometer monitoring or photogrammetric methods, would offer a cost-effective way to detect early signs of instability and guide potential mitigation efforts.

Acknowledgments: This work was supported by a VEGA grant from the Slovak Ministry of Education (contract no.1/0182/23 and no. 1/0347/25) and Slovak Research and Development Agency (VV-MVP-24-0197)

References

ASTM D5601-94, 1994: Standard test method for tearing resistance of roofing and waterproofing materials and membranes. ASTM International.

Barton N., 1976: The shear strength of rock and rock joints. International Journal of Rock Mechanics and Mining Sciences & Geomechanics Abstracts, 13, 9, 255–279.

Bell R. & Glade T., 2004: Quantitative risk analysis for landslides – Examples from Bíldudalur, NW-Iceland. Natural Hazards and Earth System Sciences, 4, 117–131.

Canuti P., Margottini C., Fanti R. & Bromhead E.N., 2009: Cultural heritage and landslides: research for risk prevention and conservation. *In:* Sassa K. & Canuti P. (Eds): Landslides—Disaster Risk Reduction. Springer, Berlin, 401–433.

Cardia S., Palma B., Langella F., Pagano M. & Parise M., 2023: Alternative methods for semi-automatic clusterization and extraction of discontinuity sets from 3D point clouds. Earth Science Informatics, 16, 2895–2914.

Cardia S., Langella F., Pagano M., Palma B., Sabato L., Tropeano M. & Parise M., 2024: 3D digital analysis for geo-structural monitoring and virtual documentation of the Saint Michael Cave in Minervino Murge, Bari (Italy). Digital Applications in Archaeology and Cultural Heritage, 32, e00308.

Cebecauer I. & Liška M., 1972: Príspevok k poznaniu krasových foriem spišských travertínov a ich kryhových zosuvov. Slovenský kras, 10. [in Slovak]

Cotecchia V., Fiorillo F., Monterisi L. & Pagliarulo R., 2005: Slope instability in the Valley of Temples, Agrigento (Sicily). Giornale di Geologia Applicata, 1, 91–101.

Fanti R., Giovanni G., Lombardi L., Deadato T. & Canuti P., 2013: Terrestrial laser scanning for rockfall stability analysis in the cultural heritage site of Pitigliano (Italy). Landslides, 10, 409–420.

Goodman R.E., 1980: Introduction to Rock Mechanics. Wiley, New York, 576 p.

Goodman R.E. & Bray J.W., 1976: Toppling of rock slopes. *In:* Proceedings of the Specialty Conference on Rock Engineering for Foundations and Slopes. ASCE, Boulder, Colorado, 2, 201–234.

Gutierrez F., 2010: Hazards associated with karst. *In:* Alcantara I. & Goudie A. (Eds): Geomorphological Hazards and Disaster Prevention. Cambridge University Press, Cambridge, 161–175.

Gutierrez F., Parise M., De Waele J. & Jourde H., 2014: A review on natural and human-induced geohazards and impacts in karst. Earth-Science Reviews, 138, 61–88.

Hoek E. & Bray J.W., 1981: Rock Slope Engineering. Revised 3rd edition. Institution of Mining and Metallurgy, London, 364 p.

Hudson J.A. & Harrison J.P., 1997: Engineering Rock Mechanics: An Introduction to the Principles and Applications. Pergamon Press, Oxford, 456 p.

Ivan L., 1943: Výskyty travertínov na Slovensku. Práce Štátneho geologického ústavu, Bratislava. [in Slovak]

ISRM, 2007: The Complete ISRM Suggested Methods for Rock Characterization, Testing and Monitoring: 1974–2006. Commission on Testing Methods, International Society for Rock Mechanics, Ankara, 628 p.

Maľa M., Greif V., Ondrášik M. & Macková A., 2021: Changes in pore characteristics of travertines from Spišské Podhradie after repeated freeze-thaw cycles. Acta Geologica Slovaca, 13, 1, 119–128.

Maľa M., Greif V. & Ondrášik M., 2024: Deterioration of volcanic tuffs from rock dwellings in Brhlovce (Slovakia) induced by freeze-thaw cycling studied by non-destructive tests and μCT visualization. Bulletin of Engineering Geology and the Environment, 83, 5, 166.

Malgot J., 1977: Deep-seated gravitational slope deformations in neovolcanic mountain ranges of Slovakia. Bulletin of the International Association of Engineering Geology, 16, 106–109.

Malgot M., Baliak F., Gregor V., Bartók J., Satina J., Kusý P., Cabala D. & Vlčko J., 1992: Spišský hrad – Inžinierskogeologický prieskum a geotechnické opatrenie. Záverečná správa. Katedra geotechniky SvF STU, Bratislava. [in Slovak]

Nemčok A., 1982: Zosuvy v slovenských Karpatoch. Veda, Bratislava, 236. [in Slovak]

Nemčok A. & Svatoš A., 1974: Gravitačný rozpad Dreveníka. Geografický časopis, 26, 3, 258–266. [in Slovak]

Nicu I.C., 2017: Natural hazards – a threat for immovable cultural heritage: A review. International Journal of Conservation Science, 8, 375–388.

Pagano M., Palma B., Ruocco A. & Parise M., 2020: Discontinuity characterization of rock masses through terrestrial laser scanner and unmanned aerial vehicle techniques aimed at slope stability assessment. Applied Sciences, 10, 2960.

Pagliarulo R. & Parise M., 2000: Landslide assessment at the archaeological site of Agrigento (Sicily, Italy). *In:* GeoEng2000 – International Conference on Geotechnical and Geological Engineering, Melbourne, Australia, 19–24 November 2000.

Pánek T. & Klimeš J., 2016: Temporal behavior of deep-seated gravitational slope deformations: A review. Earth-Science Reviews, 156, 14–38.

Parise M., Ravbar N., Živanović V., Mikszewski A., Kresic N., Mádl-Szőnyi J. & Kukurić N., 2015: Hazards in karst and managing water resources quality. *In:* Stevanović Z. (Ed.): Karst Aquifers – Characterization and Engineering. Springer, 601–687.

STN EN 1097-6, 2014: Skúšky na stanovenie mechanických a fyzikálnych vlastností kameniva. Časť 6: Stanovenie objemovej hmotnosti zŕn a nasiakavosti. Slovenský ústav technickej normalizácie, Bratislava, 41. [in Slovak]

Svatoš A., 1970: Využití leteckých snímků při inženýrsko-geologickém průzkumu svahových pohybů. ČVUT, Praha, 70. [in Czech]

Vlčko J., Greif V., Grof V., Ježný M., Petro L. & Brček M., 2009: Rock displacement and thermal expansion study at historic heritage sites in Slovakia. Environmental Geology, 58, 1727–1740.

Vítek J., 1970: Z Pekla do raja. Krásy Slovenska, 47, 11, 506–507. [in Slovak]

Zheng B., Qi S., Huang X., Guo S., Wang C., Zhan Z. & Luo G., 2020: An advanced shear strength criterion for rock discontinuities considering size and low shear rate. Applied Sciences, 10, 12, 4095.